Investigating piecewise smooth dynamical systems

Debsankha Manik

April 11, 2013

Preface

Piecewise smooth dynamical systems are of particular interest because of their ubiquity and plethora of novel behaviours. There are very elegant existing frameworks for analyzing different kinds of border collision bifurcations that occur in those systems. These include the classic work on border collision of equilibria by Feigin, analysis of grazing bifurcations using the ZDM formalism developed by Nordmark et al [**?**] and the impact map approach developed by Bernardo et al [**?**, p. 10].

Using the ZDM formalism, Banerjee and Kundu analyzed the soft impacting oscillator system and predicted the onset of chaos immediately following the grazing of a limit cycle *except* when the ratio of the damped natural frequency of the system and the forcing function frequency are in integral or half integral ratios. Experiments have roughly borne out this prediction, except for the fact that chaos has been observed to vanish in a *small neighbourhood* of those values predicted analytically. Here we have used the impact map formalism to derive the necessary conditions for chaos to vanish and matched the results with the experimental results.

It has been reported previously that the lifetimes of transients in systems exhibiting grazing bifurcations follow a power law pattern as the parameter value approaches the grazing value. We have observed the same characteristics in a simple harmonic oscillator with hard impacts. We attempt to explain this behaviour by treating the system before transients die down as an ergodic system.

# Contents

Chapter 1

Introduction

1.1 Overview

Theory of dynamical systems enables us to gain valuable insights into many problems. By using the powerful tools it provides, in many cases we can explain how a system will behave when the actual equations governing its evolution are too difficult to solve analytically. This approach has been proved time and again to be extremely useful in a diverse range of areas: fluid flows, electrical circuits, ecological systems etc.

However, conventional treatments of the subject generally places the demand that the systems be describable in terms of *smooth* functions of the dynamical variables. There are valid reasons for doing so. For a system's stability analysis, the Jacobian plays a role of paramount importance. But its existence cannot be guaranteed everywhere in the phase space for non smooth systems.

Unfortunately, many systems we need to deal with regularly are non smooth: electrical circuits involving switches, systems exhibiting sliding or chattering motion, impacting systems etc. One subclass of these systems is called *piecewise smooth* systems. The equation governing the evolution of these system changes

Figure 1.1: Trajectory of a bouncing ball : a piecewise smooth system
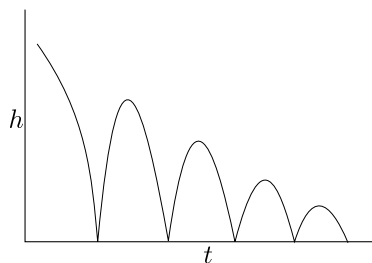
the moment the system co-ordinates cross what is known as a "switching manifold", which is a surface with dimension lower than that of the phase space. Between any two of those switches, the system evolves smoothly. For example, a ball bouncing against the floor under the influence of gravity constitutes such a system. Between any two bounces, the height of the ball h is described by $\ddot{h} = -g/m$, where g is the acceleration due to gravity and m is the mass of the ball. The solution to the equation is a parabola, as depicted in Fig 1.1, which is of course a smooth function. But at the instance of the bounce, the velocity of the ball changes changes in a non-smooth manner. Despite the simplicity of the system, it shows rich dynamical behaviour for certain parameter values [?].

1.2 Classification of piecewise smooth systems

1.2.1 Piecewise smooth maps

Definition 1.2.1. *A map described by a* finite *set of* smooth *maps:*

$$x \mapsto F_i(x, \mu) \quad \forall x \in S_i \tag{1.1}$$

is called a piecewise smooth map if:

1.

$$\begin{aligned} S_i &\in \mathbf{X} & \forall i \\ \cup_i S_i &= \mathbf{X} \\ S_i \cap S_j &= \emptyset, & i \neq j \end{aligned}$$

2. *Each of the functions F_i is smooth in both the state x and the parameter μ throughout S_i.*

Example: Tent map

$$x_{n+1} = f_\mu(x_n) = \begin{cases} \mu x_n & \text{for } x_n < \frac{1}{2} \\ \\ \mu(1 - x_n) & \text{for } \frac{1}{2} \leq x_n \end{cases} \tag{1.2}$$

Now we will define a few quantities to be used extensively in the next sections.

Definition 1.2.2. *The intersection Σ_{ij} between the closures (i.e. the set and its limit points) of any pair of S_i's are called the **switching manifolds** of the system:*

$$\Sigma_{ij} := \bar{S}_i \cup \bar{S}_j$$

Figure 1.2: Tent map
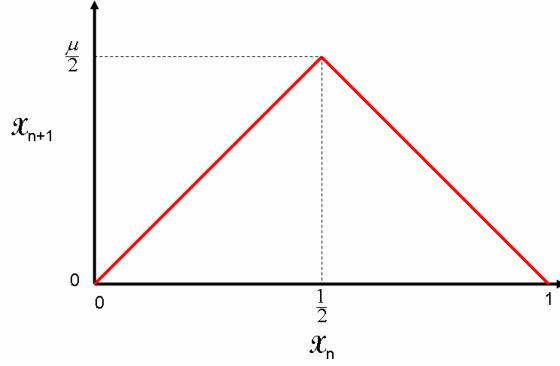
Example: In case of the Tent map (1.2), there is one switching manifold $S = 1/2$.

Definition 1.2.3. *For a point $x_0 \in \sigma_{ij}$, the leading order term in the power series expansion of $F_i(x) - F_j(x)$ about x_0 is called the **order of singularity** of the map at the point x_0.*

Example: In case of tent map,

$$F_2(x) - F_1(x) = 2\mu x - \mu \tag{1.3}$$

$$= 0 + 2\mu(x - \frac{1}{2}) \tag{1.4}$$

Therefore the order of singularity is 1.

It is obvious that if the map has a *discontinuity* at a point, the order of singularity at that point will be 0.

We will later see that piecewise smooth maps arise naturally as a result of taking Poincaré sections of *piecewise smooth flows* (Something we will define right now).

1.2.2 Piecewise smooth flows

Piecewise smooth flows are defined by extending the concept of piecewise smooth maps to continuous time systems:

Definition 1.2.4. *A flow described by a* finite *set of ODE's:*

$$\dot{x} = F_i(x, \mu) \qquad \forall x \in S_i \tag{1.5}$$

is called a piecewise smooth flow if:

1.

$$
\begin{aligned}
S_i &\in \mathbf{X} & \forall i \\
\cup_i S_i &= \mathbf{X} \\
S_i \cap S_j &= \emptyset, & i \neq j
\end{aligned}
$$

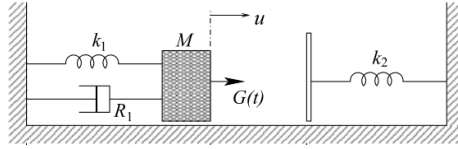2. *Each of the vector fields F_i is smooth in both the state x and the parameter μ throughout S_i.*

3. *Each of the vector fields F_i admits a solution $\varphi_i(x)$:*

$$
\dot{\varphi}_i(x,t)|_{t=0} = F_i(x) \quad \forall x \in S_i \tag{1.6}
$$

that is smooth in both the state x and the parameter μ throughout S_i.

Figure 1.3: Impact oscillator

Example: Oscillator with soft impacts

Consider a simple harmonic oscillator driven by a driving force $G(t)$ which hits against another spring attached to the wall at a distance σ from its equilibrium position. The equation of motion is given by:

$$
m\ddot{x} = \begin{cases} -\gamma\dot{x} - k_1 x + G(t) & \text{for} \ \ x < \sigma \\[2mm] -\gamma\dot{x} - k_1 x - k_2(x - \sigma) + G(t) & \text{for} \ \ x \geq \sigma \end{cases} \tag{1.7}
$$

Switching manifolds of piecewise smooth flows are defined identically to those of piecewise smooth maps (1.2.2), while order of singularities are defined slightly differently:

Definition 1.2.5. *For a point $x_0 \in \Sigma_{ij}$, the first non zero partial derivative of $\varphi_i(x_0,t) - \varphi_j(x_0,t)$ with respect to t at $t = 0$ is called the **order of singularity** of the flow at the point x_0.*
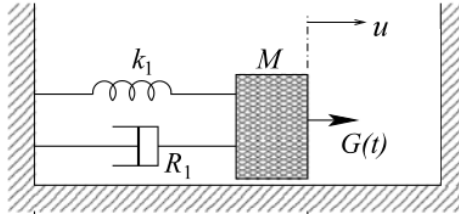
1.2.3 Piecewise smooth hybrid systems

Definition 1.2.6. *A system described by a set of ODE's and a set of* **reset maps***:*

$$\dot{x} = F_i(x, \mu), \quad \forall x \in S_i \tag{1.8}$$

$$s \mapsto R_{ij}(x, \mu), \quad \forall x \in \Sigma_{ij} = \bar{S}_i \cup \bar{S}_j \tag{1.9}$$

is called a piecewise smooth hybrid system if all the R_i's, F_i's as well as the associated flows φ_i's are smooth in both x and the parameter μ in the appropriate regimes.

Figure 1.4: Hard impacting oscillator

Example: Oscillator with hard impacts

Consider a driven simple harmonic oscillator with a hard wall at a distance σ from its equilibrium position. The equation of motion is:

$$m\ddot{x} = -\gamma\dot{x} - k_1 x + G(t) \qquad \text{for} \quad x < \sigma \tag{1.10}$$

$$(x, v) \mapsto (x, -rv) \qquad \text{for} \quad x = \sigma \tag{1.11}$$

Where r is the coefficient of restitution, which is 1 for perfectly elastic collisions.

1.3 Bifurcations in piecewise smooth systems

Piecewise smooth dynamical systems, quite naturally, can show all the usual types of dynamical behaviour shown by smooth dynamical systems : period doubling [**?**, p. 166-170] bifurcations, saddle-node [**?**, p. 109] bifurcations etc.

However, piecewise smooth systems exhibit a plethora of interesting behaviours which involve the sudden change in the system dynamics at the switching manifolds and hence, which are not possible in smooth systems. An extensive mathematical framework to study these behaviours was first published in the Russian literature as early as the seventies of the last century by Mark Feigin [**?**]. Then these types of behaviours were named *C-bifurcations*. Now they also go by the name of *border collision bifurcations*. We will briefly review a few of these novel behaviours now.

Figure 1.5: A few cases of border collision bifurcations

Bifurcation of equillibria   Grazing bifurcation

Sliding bifurcation
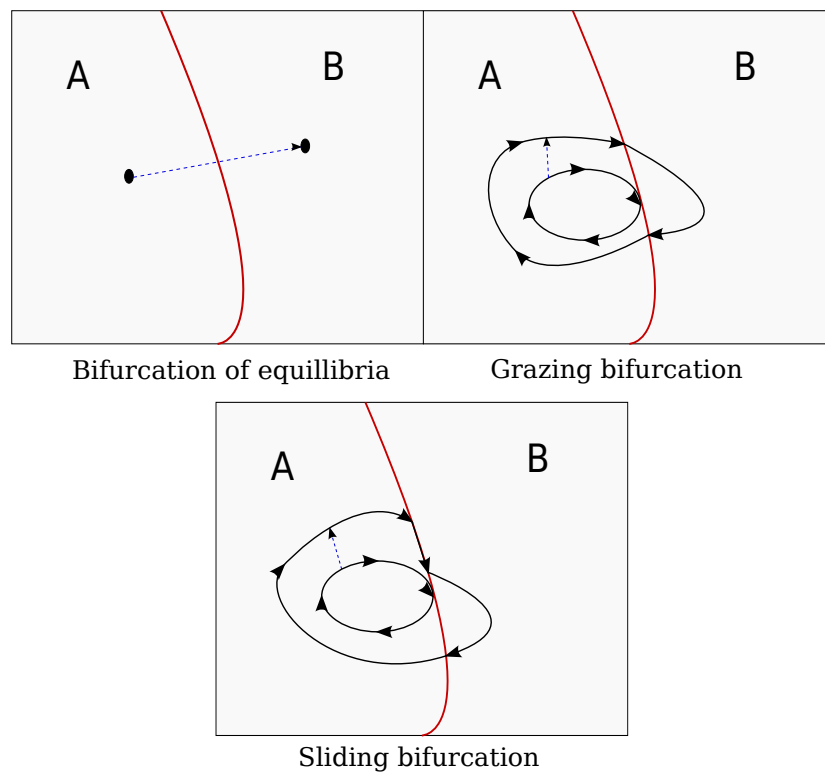
1.3.1   Border collision of equilibria

Consider a piecewise smooth map:

$$\dot{\mathbf{x}} = \begin{cases} F_1(\mathbf{x}) & : H(\mathbf{x}) < 0 \\ F_2(\mathbf{x}) & : H(\mathbf{x}) > 0 \end{cases} \qquad (1.12)$$

Where $H(x) = 0$ defines the switching manifold:

$$S_1 = \{x : H(x) < 0\}$$
$$S_2 = \{x : H(x) \geq 0\}$$

Suppose there exists an equilibrium point of the piecewise smooth system $x_1^*(\mu)$ in the region S_1 of the phase space:

$$F_1(x_1^*(\mu)) = 0$$

Now, as the parameter μ is changed, this point will, in general, move in the phase space. Sometimes it may happen that for parameter values $\mu > \mu_0$ this point $s_1^*(\mu)$ crosses the boundary and lands up in the region S_2. But in that region $\dot{x} = F_1(x)$ is *not the correct ODE in the first place*! Therefore $x_1^*(\mu)$ is no longer a fixed point. We call it a **virtual fixed point** of the system and such a phenomenon is called "border collision of equilibrium". This phenomenon was first studied by Marc Feigin in case of discrete time systems [**?**](later extended by Bernardo *et al* to continuous time systems [**?**]) where he classified the dynamical behaviours that can take place when equilibria crosses the switching manifold and derived the necessary conditions for each of them in terms of the eigenvalues of the Jacobians at both sides of the switching manifold. We will now briefly discuss this approach.

Types of border collision of equilibria

Consider a piecewise smooth flow described by (1.12). Let's switch to a coordinate system such that the equations of motion look like:

$$\dot{\mathbf{x}} = \begin{cases} F_1(\mathbf{x}, \mu) & : x_n < 0 \\ F_2(\mathbf{x}, \mu) & : x_n \geq 0 \end{cases} \qquad (1.13)$$

(Where x_n denotes the n-th component of $\mathbf{x}$.)

Suppose that for every value of the parameter μ, $\exists$ two fixed points of the flow, one in each side of the switching manifold:

$$F_1(\mathbf{x_1^*}, \mu) = 0, \ \ x_{1n}^* \leq 0 \qquad (1.14)$$
$$F_2(\mathbf{x_2^*}, \mu) = 0, \ \ x_{2n}^* \leq 0 \qquad (1.15)$$

We can also assume without loss of generality that the border collision takes place for the parameter value $\mu = 0$ at the point $\mathbf{x} = 0$:

$$\mathbf{x_1^*} = \mathbf{x_2^*} = \mathbf{0} \ \text{ if } \mu = 0$$

Then we can locally linearize the map:

$$\dot{\mathbf{x}} = \begin{cases} \mathbf{A_1}\mathbf{x} + \mathbf{B}\mu & : x_n < 0 \\ \mathbf{A_2}\mathbf{x} + \mathbf{B}\mu & : x_n < 0 \end{cases}$$

Where:

$$\mathbf{A_i} = \frac{\partial \mathbf{F_1}}{\partial \mathbf{x}}\bigg|_{\mathbf{x}=\mathbf{0}}$$

and

$$\mathbf{B} = \frac{\partial \mathbf{F_1}}{\partial \mu}\bigg|_{\mu=\mathbf{0}} = \frac{\partial \mathbf{F_2}}{\partial \mu}\bigg|_{\mu=\mathbf{0}}$$

(Assuming the flow to be continuous at $\mathbf{x} = 0$).

Also, $\mathbf{A_1}$ and $\mathbf{A_2}$ can differ only in the $n-$th column (Again due to continuity, this time at $\mu = 0$).

Now (1.14) becomes:

$$A_1\mathbf{x_1^*} + \mathbf{B}\mu = 0 \tag{1.16}$$
$$A_2\mathbf{x_2^*} + \mathbf{B}\mu = 0 \tag{1.17}$$

Assuming A_i's are invertible:

$$\mathbf{x}_i^* = -\mathbf{A_i}^{-1}\mathbf{B}\mu = -\frac{adj(\mathbf{A_i})}{det(\mathbf{A_i})}\mathbf{B}\mu \tag{1.18}$$

The fixed points $\mathbf{x}^*_i$ will be real iff

$$x_{1_{n<0}}^* < 0, x_{2_n}^* > 0.$$

Now, from (1.18)

$$x_{1_k}^* = \frac{c_{1_k}^*}{det(\mathbf{A_1})}\mu, x_{2_k}^* = \frac{c_{2_k}^*}{det(\mathbf{A_2})} \tag{1.19}$$
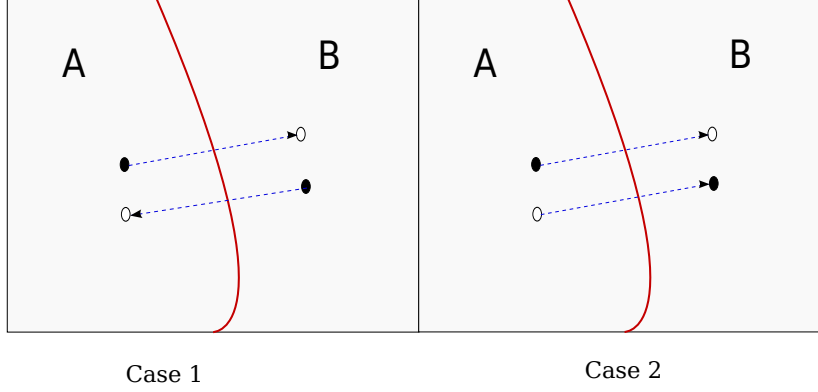
Where,

$$c_{i_k}^* = [-adj(\mathbf{A_i})\mathbf{B}]_{\mathbf{k}}$$

Because A_1 differs from A_2 only in $n-$th column, $c_{1_n}^* = c_{2_n}^* := C$

Therefore we have:

$$x_{1_n}^* = \frac{C}{det(\mathbf{A_1})}\mu, x_{2_k}^* = \frac{C}{det(\mathbf{A_2})}\mu \tag{1.20}$$

Figure 1.6: Border collision of equilibria

Case 1   Case 2

Cases:

1. $det(\mathbf{A_1})det(\mathbf{A_1}) < 0$: $x^*_{1_n}$ and $x^*_{2_n}$ always have opposite signs: In that case, before border collision, there'd be 2 real fixed points in opposite sides of the switching manifold. As the parameter is changed, they'd *simultaneously* suffer border collision and become virtual fixed points.

2. $det(\mathbf{A_1})det(\mathbf{A_1}) > 0$: $x^*_{1_n}$ and $x^*_{2_n}$ always have same signs: In that case, initially $\mathbf{x}^*_1$ will be real and $\mathbf{x}^*_2$ virtual (or vice versa), and after border collision $\mathbf{x}^*_1$ will become virtual and $\mathbf{x}^*_2$ real.

Period doubling at border collision of equilibria

Sometimes it may happen that after a fixed point undergoes border collision, a period-2 orbit emerges. This phenomenon was also studied in great detail by [**?**]. Here we discuss in brief a very important necessary condition for this to happen.

Claim 1.3.1. *Consider a piecewise smooth map of the form* (1.1)*:*

$$x_{n+1} = f(x_n, \mu) = \begin{cases} f_1(x_n, \mu) & \text{for} \quad x_n < 0 \\ \\ f_2(x_n, \mu) & \text{for} \quad x_n \geq 0 \end{cases} \tag{1.21}$$

Suppose ∃ *a fixed point of the map* $x^*_1 < 0$ *so long as the parameter* $\mu < 0$. *Suppose that when* μ *equals* 0, x^*_1 *suffers border collision and increasing* μ *further, a period-doubling bifurcation occurs. Then the Jacobian of the map must suffer a discontinuity at* 0, *the point of border collision at the parameter value* $\mu = 0$
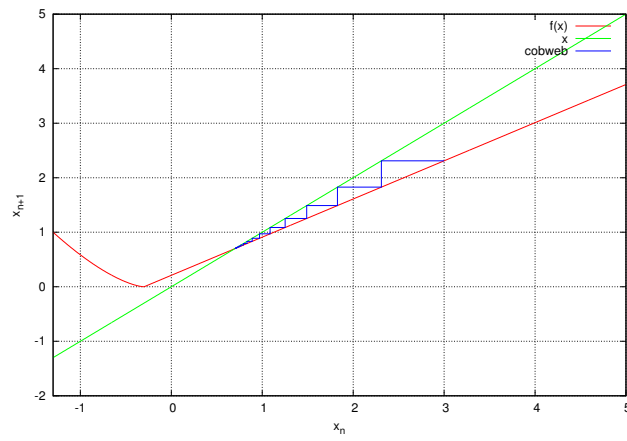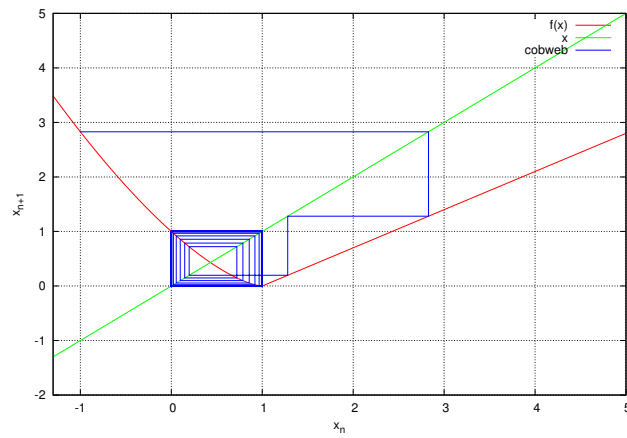
Figure 1.7: Before border collision: period 1

Figure 1.8: After border collision: period 2

Proof. Here we will consider the 1-dimensional case. A period doubling bifurcation occurs if on changing the parameter value of a system,

1. The fixed point of the first composition of the map either no longer exists or loses stability.

2. A fixed point in the second composition of the map either gets created or becomes stable.

Suppose that after border collision, this period-2 orbit is now stable:

$$f_1(x_1) = x_2, \quad x_1 < 0$$
$$f_2(x_2) = x_1$$

For stability, the derivative of the second composition must be less than 1 in magnitude:

$$\left| \frac{d}{dx} f_2(f_1(x_1)) \right| < 1$$
$$|f_1'(x_1) f_2'(x_2)| < 1$$

Now, immediately after border collision, $0 < \mu \ll 1$, the period-2 orbit will be very close to the original period-1 fixed point: $-1 \ll x_1 < 0, 0 < x_2 \ll 1$. Therefore

$$|f_1'(0) f_2'(0)| < 1$$

Now, supposing the Jacobian suffers no discontinuity, this condition can be satisfied only if:

$$|f_1'(0)| < 1, |f_2'(0)| < 1 \tag{1.22}$$

But if that is the case, then the fixed point of the *first composition* of the map (which was an attractor before the border collision and since the map is assumed to be continuous in the parameter μ, is still in a neighbourhood of 0), is still an attractor. But this contradicts the necessary condition for a period doubling bifurcation (i.e. the fixed point of the first composition must lose stability). Therefore condition (1.22) can only be satisfied if the Jacobian suffers a discontinuity at border collision.

For a more rigorous proof applicable for systems of any dimensionality, please refer to [?].

□

1.3.2 Grazing bifurcation of limit cycles due to border collision

The phenomenon of a limit cycle grazing the switching manifold of a system is encountered very frequently. These systems have been studied extensively by Dankowicz and Nordmark [?], Bernardo at al [?], Banerjee and Kundu [?] etc.

Consider a piecewise smooth flow as defined in (1.5):

$$\dot{x} = \begin{cases} F_1(x) & H(x) \leq 0 \\ F_2(x) & H(x) > 0 \end{cases} \tag{1.23}$$

Suppose there exists an orbit (henceforth assumed to be period-1, for sake of simplicity) which grazes against the switching manifold defined by the equation $H(x) = 0$ at a point 0. By construction, $H(0) = 0$. Now we'd like to know how initial conditions starting very close to this stable grazing orbit behave. There exists a very powerful method of analyzing the stability of closed orbits of flows which goes like this:

1. Take a Poincaré section, which is basically a plane P with dimensionality 1 less than that of the phase space. Especially in case of systems driven by an external periodic force with time period T, this section is generally taken by looking at the system at $t = nT$ (the so-called *stroboscopic Poincaré section*). Suppose the closed orbit intersects this Poincaré plane at a point x_0.

2. Now choose a point x_1 very close to x_0 and see where it lands up on the Poincaré plane after time T. This will define a so-called **Poincaré map**

$$\Pi : P \to P$$

3. By construction, x_0 is a fixed point of the map Π. Hence it can be locally linearized:
$$\Pi(x) - x_0 \approx J(x_0)(x - x_0)$$

   Where $J = \frac{\partial \Pi}{\partial x}$.

4. The eigenvalues of the Jacobian determine the stability of the grazing orbit. If all the eigenvalues are < 1 is magnitude then it is stable, otherwise not.

As depicted in Fig 1.9, when grazing takes place, certain initial conditions close to the grazing orbit give rise to non-impacting orbits and others give rise to impacting orbits.

Let a very important fact be noted here: *The Poincaré map derived from a piecewise smooth flow will be a piecewise smooth map*: the switching manifold being the collection of points $x^* \in P$ such that orbits starting from them grazes the switching manifold of the actual flow.

As we showed in Claim 1.3.1, the Jacobian so obtained will have to be discontinuous across the switching manifold for a period doubling cascade to take place after grazing.

In the next section we will discuss a way of obtaining the Poincaré map Π for piecewise smooth flows: the ZDM method.

Figure 1.9: Grazing orbit
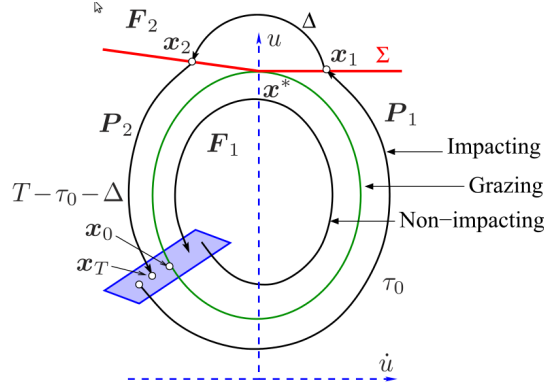
1.4 Literature survey

1.4.1 ZDM

Consider the piecewise smooth flows defined by (1.12).Suppose there exists a grazing orbit in the region $H(x) > 0$ that grazes the switching manifold at the point $x = 0$. We impose the following restrictions on the system and the grazing orbit:

1. $H(0) = 0$ (A necessary condition for $x = 0$ to be a grazing point).

2. $\frac{dH}{dx} \neq 0$ (Ensuring H varies smoothly with x, a property to be used later).

3. $\frac{d}{dt} H(\varphi_i(0, t))|_{t=0} = 0$ (Assuming both the vector fields are tangential to the switching manifold).[1]

4. $a_i^* := \frac{d^2}{dt^2} H(\varphi_i(0, t))|_{t=0} > 0$ (Ensuring that $H(x)$ attains a minimum value for any orbits close to 0, another property to be used later.)

Consider an orbit starting from a point x_i which is close to a grazing orbit (See Fig 1.10). Suppose the orbit spends time δ_0 to hit the switching manifold at the point x_1, then it evolves according to the second vector field F_2. After time δ, it reaches the point with minimum H, an occurrence guaranteed by property 4. After time δ' , it hits the switching manifold again at point x_2

The ZDM is defined as a map which maps x_i to a point x_3 in zero time such the time taken to go from x_i to x_2 equals the time *it would have taken to go* from x_3 to x_2, if the motion were governed by the vector field F_1. From Fig

---

[1] $\dot{\varphi}_i(x, t)|_{t=0} = F_i(x)$. $\varphi_i(x, t)$ denotes an orbit satisfying the corresponding ODE starting from the initial co-ordinate x at $t = 0$.

Figure 1.10: ZDM

1.10, it is evident that

$$ZDM(x_i) = \varphi_2(-\delta_0 - \delta - \delta', x_2)$$

The advantage of the ZDM formalism is that any orbit starting from the point x_i at time 0 and ending at a point x_f at time t, both in the region $H(x) > 0$ and involving a single foray into the 'other' side side of the flow can be written as:

$$x_f = \varphi_1(ZDM(x_i), t) \tag{1.24}$$

In particular, ZDM approach enables one to calculate the stroboscopic poincare maps for orbits shown in Fig 1.9:

$$\Pi(x_i) = \varphi_1((ZDM(\varphi_1(x_i, \tau_0)), T - \tau_0) \tag{1.25}$$

after which stability analysis becomes possible using the usual method of calculating the eigenvalues of the jacobian of Π at the fixed point.

1.4.2   Narrow band chaos

Impact oscillators as described in (1.7) and (1.10) have been studied extensively since the 1970's when Feigin [?] described their bifurcation structure. We now know that they can exhibit extremely rich dynamical behaviour. Using the ZDM approach, Banerjee et al [?] investigated the grazing bifurcations in such systems. They found that the Jacobian suffers a discontinuity at grazing (which, as we showed in Claim 1.3.1, is a necessary condition for period doubling bifurcation at grazing) *unless* the damped natural frequency of the system is an integral multiple of half the frequency of the external driving force:
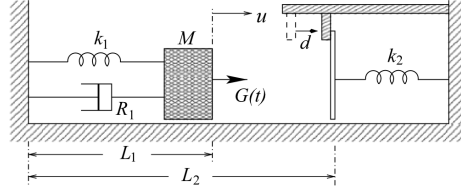
$$n = \frac{2\omega_g}{\omega_{forcing}} \in \mathbb{N} \tag{1.26}$$

This implies that chaos initiated by a period doubling cascade cannot take place at those specific n-values. Now we will describe their method.

ZDM for soft impacting oscillator

Figure 1.11: Oscillator with soft impact

The system is depicted in Fig 1.4.2. The equations of motion are:

$$m\ddot{x} = \begin{cases} -\gamma\dot{x} - k_1 x + G(t) & \text{for } x < \sigma \\ \\ -\gamma\dot{x} - k_1 x - k_2(x - \sigma + d) + G(t) & \text{for } x \geq \sigma \end{cases} \tag{1.27}$$

Since this is a non-autonomous[2] system defined by a second order ODE, we can write in in an autonomous first order form by defining the state variable as a 3-dimensional vector:

$$\mathbf{x} = \begin{pmatrix} x \\ v \\ t \end{pmatrix} \tag{1.28}$$

as the equations of motion then become:

$$\dot{\mathbf{x}} = \begin{pmatrix} \dot{x} \\ \dot{v} \\ \dot{t} \end{pmatrix} = \begin{cases} F_1(\mathbf{x}) = \begin{pmatrix} v \\ (-\gamma v - k_1 x + G(t))/m \\ 1 \end{pmatrix} & \text{for } x < \sigma \\ \\ F_2(\mathbf{x}) = \begin{pmatrix} v \\ (-\gamma v - k_1 x - k_2(x - \sigma + d) + G(t))/m \\ 1 \end{pmatrix} & \text{for } x \geq \sigma \end{cases} \tag{1.29}$$

At suitable parameter values, there will be grazing and impacting orbits as depicted in Fig 1.9. In that case, we can analyze the system dynamics in terms of a Poincaré map taking the form:

$$\Pi = N_2 \circ ZDM \circ N_1 \tag{1.30}$$

Where N_1 is a state transition matrix that takes a point x_i on the Poincaré plane to the switching manifold and N_2 is the state transition matrix that takes the result of applying the ZDM back to the Poincaré plane.

N_1 and N_2 can be obtained from the solution of the driven SHO, which can be analytically solved. So ZDM is the only tricky part.

---

[2]i.e. explicitly depending on time

Figure 1.12: Calculating the ZDM

$$ZDM : x_1 \mapsto x_3$$
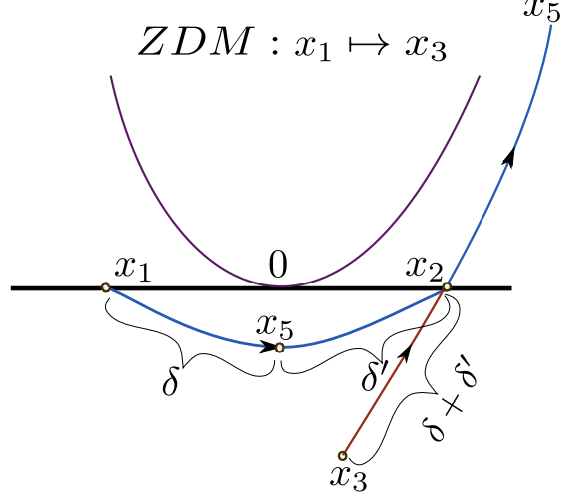
As we can see from Fig 1.12, the calculation ^{3} involves deriving expressions for δ and δ' as a function of x_1 first.

Calculate δ:

$$x_1 = \varphi(x_5, -\delta)$$

$$H(x_1) = H(\varphi(x_5, -\delta))$$

$$\approx H(\varphi_2(x_5, 0)) + \frac{\partial}{\partial t} H(\varphi_2(t, x_5)) \mid_{t=0} (-\delta)$$

$$+ \frac{\partial^2}{\partial t^2} H(\varphi_2(t, x_5)) \mid_{t\approx 0} \frac{\delta^2}{2}$$

$$\approx H(x_5) + 0 + \frac{\partial^2}{\partial t^2} H(\varphi_2(t, 0)) \mid_{t\approx 0} \frac{\delta^2}{2}$$

$$\approx H(x_5) + a_2^* \frac{\delta^2}{2}$$

Let $H(x_5) = H_{min}(x_i) = -y^2$:

$$\delta = y\sqrt{\frac{2}{a_2^*}} \tag{1.31}$$

Calculate ZDM: Using identical arguments, $\delta' = y\sqrt{\frac{2}{a_2^*}}$

Let $\delta + \delta' = \delta_1$

---

^{3}Notice that since we are calculating the ZDM of a point *on* the switching manifold, calculations are simpler than the general case depicted in Fig 1.10

Then:

$$x_3 \approx x_2 - F_1(x_2)\delta_1 + \dot{F}_1(x_2)\frac{\delta_1^2}{2} - \ddot{F}_1(x_2)\frac{\delta_1^3}{6} \tag{1.32}$$

$$x_1 \approx x_2 - F_2(x_2)\delta_1 + \dot{F}_2(x_2)\frac{\delta_1^2}{2} - \ddot{F}_2(x_2)\frac{\delta_1^3}{6} \tag{1.33}$$

$$x_3 = x_1 - (F_1 - F_2)(x_2)\delta_1 + (\dot{F}_1 - \dot{F}_2)(x_2)\frac{\delta_1^2}{2} - (\ddot{F}_1 - \ddot{F}_2)(x_2)\frac{\delta_1^3}{6} \tag{1.34}$$

$$\approx x_1 - (F_1 - F_2)(x^*)\delta_1 + \text{H.O.T.} \tag{1.35}$$

Now we go back to the definitions of F_i for the impact oscillator (1.29) and notice:

$$F_2(x) - F_1(x) = \begin{pmatrix} v \\ (-\gamma v - k_1 x - k_2(x - \sigma + d) + G(t))/m \\ 1 \end{pmatrix} - \begin{pmatrix} v \\ (-\gamma v - k_1 x + G(t))/m \\ 1 \end{pmatrix} \tag{1.36}$$

$$= \begin{pmatrix} 0 \\ k_2(-x + \sigma - d)/m \\ 0 \end{pmatrix} \tag{1.37}$$

Here $x^* = \sigma$. Therefore $F_2(x^*) - F_1(x*) = Q \begin{pmatrix} 0 \\ 1 \\ 0 \end{pmatrix}$, where $Q = -k_2 d/m$.

Thus we have from (1.34):

$$ZDM(\mathbf{x}) = \mathbf{x} - (F_1 - F_2)(x^*)\delta_1 \tag{1.38}$$

$$= \mathbf{x} + 2Q\sqrt{\frac{-2H_{min}(x)}{a_2^*}} \begin{pmatrix} 0 \\ 1 \\ 0 \end{pmatrix} \tag{1.39}$$

Calculating the Jacobian of the Poincaré map   For orbits close to grazing, the total Poincaré map would be given by (1.30). Therefore the Jacobian J of the map would be:

$$J = J_{N_2} \cdot J_{ZDM} \cdot J_{N_1} \tag{1.40}$$

Jacobian of the ZDM   From (1.38), we get:

$$J_{ZDM} = \begin{pmatrix} 1 & 0 & 0 \\ \alpha & 1 & 0 \\ 0 & 0 & 1 \end{pmatrix} \tag{1.41}$$

Where $\alpha = -Q\sqrt{\frac{a^*}{-2H_{min}(x)}} H'_{min}(x)$

Here it should be noted that at grazing $H_{min} = \sigma - \sigma = 0$. Therefore we see that the Jacobian of the ZDM will have a singularity at grazing. This singularity will be seen to be the root of the discontinuity in the Jacobian, which in turn, will cause the period doubling cascade.

Jacobian of N_i
By definition,

$$N_1(\mathbf{x}) = e^{A\tau}\mathbf{x} \quad \left[\text{Where } A = \begin{pmatrix} 0 & 1 & 0 \\ -k_1/m & -\gamma/m & 0 \\ 0 & 0 & 1 \end{pmatrix}\right] \tag{1.42}$$

$$= \frac{e^{-\gamma t/2}}{\omega_g} \begin{pmatrix} \omega_g \cos\omega_g t + \frac{\gamma}{2}\sin\omega_g t & \sin\omega_g t & 0 \\ -k\sin\omega_g t & \omega_g \cos\omega_g t - \frac{\gamma}{2}\sin\omega_g t & 0 \\ 0 & 0 & 1 \end{pmatrix} \mathbf{x} \tag{1.43}$$

Where $\omega_g = \frac{\sqrt{4k-\gamma^2}}{2}$
Similarly,

$$N_2(\mathbf{x}) = e^{A(T-\tau)}\mathbf{x}$$

Therefore

$$J_{N_1} = e^{A\tau} := e^{-\gamma\tau/2} \begin{pmatrix} n_{11} & n_{12} & 0 \\ n_{13} & n_{14} & 0 \\ 0 & 0 & 1 \end{pmatrix} \tag{1.44}$$

and

$$J_{N_2} = e^{A(T-\tau)} := e^{-\gamma(T-\tau)/2} \begin{pmatrix} n_{21} & n_{22} & 0 \\ n_{23} & n_{24} & 0 \\ 0 & 0 & 1 \end{pmatrix} \tag{1.45}$$

Now we are in a position to investigate the discontinuity of the Jacobian. We first note that the Jacobian of all three parts of the map, although 3×3 in dimension, behaves like identity on the third co-ordinate, the time. Hence it is essentially a 2×2 determinant. And it has been shown by Banerjee and Grebogi that any $2-$D map can, by means of a suitable co-ordinate transformation, be written in the form:

$$M = \begin{pmatrix} a & b \\ c & d \end{pmatrix} = \begin{pmatrix} Tr(M) & 1 \\ -det(M) & 0 \end{pmatrix}$$

From (1.44) and (1.45) it can be easily shown that

$$det(J_{N_1}) = e^{-\gamma\tau/2}, det(J_{N_2}) = e^{-\gamma(T-\tau)/2}$$

Also, from (1.38),

$$det(J_{ZDM}) = 1$$

Therefore it is evident the determinant of the Poincaré map does not suffer any discontinuity.

Now we will look at the trace.

Using (1.40):

$$J = e^{-\gamma T/2} \begin{pmatrix} n_{21} & n_{22} & 0 \\ n_{23} & n_{24} & 0 \\ 0 & 0 & 1 \end{pmatrix} \begin{pmatrix} 1 & 0 & 0 \\ \alpha & 1 & 0 \\ 0 & 0 & 1 \end{pmatrix} \begin{pmatrix} n_{11} & n_{12} & 0 \\ n_{13} & n_{14} & 0 \\ 0 & 0 & 1 \end{pmatrix} \tag{1.46}$$

$$= e^{-\gamma T/2} \begin{pmatrix} n_{21} & n_{22} & 0 \\ n_{23} & n_{24} & 0 \\ 0 & 0 & 1 \end{pmatrix} \begin{pmatrix} n_{11} & n_{12} &) \\ \alpha n_{11} + n_{13} & \alpha n_{12} + n_{14} & 0 \\ 0 & 0 & 1 \end{pmatrix} \tag{1.47}$$

Therefore

$$Tr(J) = e^{-\gamma T/2}(n_{11}n_{21} + n_{13}n_{22} + \alpha(n_{11}n_{22} + n_{12}n_{24}) + n_{12}n_{23} + n_{14}n_{24} + 1) \tag{1.48}$$

Obviously, α is the only term that contains the singularity term in the form of $H_{min}^{-1/2}$. We take a closer look at the coefficient of α.

From (1.44) and (1.45):

$$n_{11} = \left\{ \omega_g \cos \omega_g \tau + \frac{\gamma}{2} \sin \omega_g \tau \right\} / \omega_g \tag{1.49}$$

$$n_{22} = \left\{ \sin \omega_g (T - \tau) \right\} / \omega_g \tag{1.50}$$

$$n_{12} = \left\{ \sin \omega_g \tau \right\} / \omega_g \tag{1.51}$$

$$n_{24} = \left\{ \omega_g \cos \omega_g (T - \tau) - \frac{\gamma}{2} \sin \omega_g (T - \tau) \right\} / \omega_g \tag{1.52}$$

Therefore the term with possible discontinuity is

$$\alpha \frac{\sin \omega_g T}{\omega_g} \tag{1.53}$$

$$= \alpha \frac{\sin 2\pi \frac{\omega_g}{\omega}}{\omega_g} \tag{1.54}$$

This equation has a serious ramification: the discontinuity vanishes if

$$\frac{2\omega_g}{\omega} \in \mathbb{N}. \tag{1.55}$$

According to our Claim 1.3.1, when the two frequencies are at these exact ratio, there won't be any period doubling cascade on grazing.
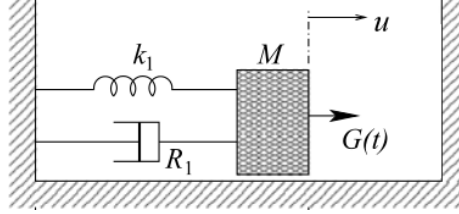
1.4.3 Impact map

Consider the impact oscillator system described by (1.10)

$$m\ddot{x} = -\gamma \dot{x} - k_1 x + G(t) \qquad \text{for} \quad x < \sigma \tag{1.56}$$

$$(x, v) \mapsto (x, -rv) \qquad \text{for} \quad x = \sigma \tag{1.57}$$

Where r is the coefficient of restitution.

Figure 1.13: Oscillator with hard impacts

In such a system, quite often periodic orbits are observed which involve one or more impacts at the hard wall at $x = \sigma$. For simplicity, let's consider orbits with only one collision. Clearly, one necessary condition for such orbits to exist is:

$$(\sigma, v) \overset{nT}{\mapsto} (\sigma, -v/r)$$

Where nT is the time period of the orbit. This map is known as the *impact map*. For a stable orbit, apart from this equation, the Jacobian should have eigenvalues with absolute values < 1. This approach was used in [?, Ch. 2; p. 20], where they obtained the necessary conditions for saddle-node and period-doubling grazing bifurcations to occur in impact oscillators without damping.

1.4.4 Numerical computation of fixed points

The method of impact map works very well to solve for periodic orbits involving only one collision per cycle (termed $PnC1$ orbits)[4] with the hard wall. But this method does not work well for parameters values for which stable orbits collide multiple times in a single cycle. Ma et al [?] devised a way to numerically compute any stable or unstable $PnCm$ orbit. We explain the method below.

For simplicity, we supposing the orbit crosses the border only once, although the strength of this approach is in finding more complicated orbits. Such an orbit is depicted in Fig 1.14. Then finding out the orbit boils down to finding out the solution to this set of equations:

$$x_1 = \varphi_1(x_0, 0, \tau_0) \tag{1.58}$$
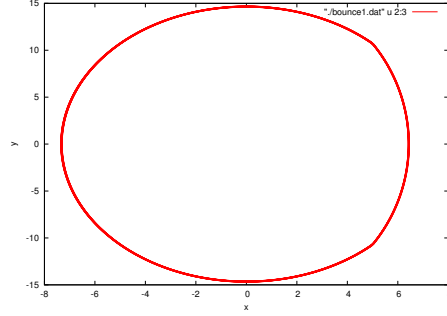$$H(x_1) = 0 \tag{1.59}$$
$$x_2 = \varphi_2(x_1, \tau_0, \tau_1) \tag{1.60}$$
$$H(x_2) = 0 \tag{1.61}$$
$$x_0 = \varphi_1(x_2, \tau_1, T - \tau_0 - \tau_1) \tag{1.62}$$

This is a set of $3n + 2$ equations in $3n + 2$ unknowns, so this can be tackled

---

[4]n signifies the periodicity of the orbit

Figure 1.14: A $P1C1$ orbit

with standard Newton's method of root finding:

$$y_{n+1} = \frac{G(y_n)}{J(\bar{y}_n)}$$

Here $y := \{x_0, x_1, x_2, \tau_0, \tau_1\}$ is a $3n + 2$ dimensional vector.

Thus we can use the standard methods of stability analysis by evaluating the eigenvalues of the Jacobian at the fixed points.

1.4.5 Lifetime of transients

The problem of long lived transients plagues many nonlinear systems. Despite the existence of a stable fixed point, trajectories starting from many initial conditions are found to take a lot of time to reach the fixed point. In case of systems involving grazing, Grebogi et al. [?] predicted that in a system where grazing occurs at parameter value $\rho = \rho_c$, average transient lifetimes vary as

$$\tau \propto |\rho - \rho_c|^{-\gamma} \tag{1.63}$$

Where the value γ is called the critical transient of the system. They derived an analytical expression for γ in terms of the eigenvalues of the Jacobian at the fixed points of the system.

1.5 Scope of present work

As we described in Subsection 1.4.2, Banerjee et al. predicted by calculating the ZDM that chaos through on border collision route should not happen in soft impacting oscillators if $2\omega_g/\omega \in \mathbb{N}$. The same analysis was found out to hold for hard impacting oscillators in [?], Experimental results were found to match this prediction very well. However, chaos was seen to vanish not only when n were exactly integers, but in a small neighbourhood of each of them. So far, no

explanation for this has been published. In the next chapter, we will take up this problem.

During our simulations on hard impacting oscillators, we observed transients orders of magnitude longer than what should take place in a corresponding system without the nonlinearity imposed by the impacts. No study on transient lifetimes in impacting systems had been published so far. It needs to be checked if the results of Grebogi et al. [?], derived for maps, holds true for continuous time impacting systems or not and if it does, whether a way to compute the critical exponent could be devised.

Chapter 2

Our system

As promised in the last chapter, we will now investigate two problems: the vanishing of chaos in hard impacting oscillator and the problem of long transients in the same system.

2.1   Description

We briefly describe our system again.

Figure 2.1: Hard impacting oscillator
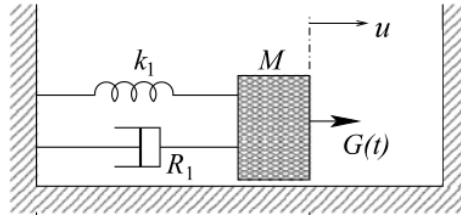
It consists of a driven simple harmonic oscillator with a hard wall at a distance σ from its equilibrium position. The equation of motion is:

$$m\ddot{x} = -\gamma\dot{x} - k_1 x + F\cos\omega t \qquad \text{for } x < \sigma \qquad (2.1)$$
$$(x, v) \mapsto (x, -rv) \qquad \text{for } x = \sigma \qquad (2.2)$$

Where r is the coefficient of restitution, which is 1 for perfectly elastic collisions. In the rest of the thesis, we will assume all the collisions to be perfectly elastic unless explicitly stated otherwise.

2.1.1   Solution disregarding the boundary

If we forget the boundary for a moment, the equation of motion is a non-homogeneous ODE. As usual, its solution is a sum total of a *homogeneous solution* and a *particular solution*:

$$x(t) = x_p(t) + x_h(t) \tag{2.3}$$

$$x_p(t) = \frac{F/m}{\sqrt{(\omega_0^2 - \omega^2)^2 + \omega^2\gamma^2}} cos(\omega t + tan^{-1}\frac{\omega\gamma}{\omega^2 - \omega_0^2}) \tag{2.4}$$

$$x_h(t) = \frac{e^{-\gamma t/2}}{\omega_g} \left\{ (\omega_g \cos\omega_g t + \frac{\gamma}{2}\sin\omega_g t)x(0) + (\sin\omega_g t)v(0) \right\} \tag{2.5}$$

$$\omega_g = \sqrt{\omega_0^2 - \frac{\gamma^2}{4}} \tag{2.6}$$

Here it should be noted that only the homogeneous solution contains the dependence on the initial conditions.

2.2   Approximate Poincaré map

In this section we will make an attempt to derive an expression for a Poincaré map for our system assuming $PnC1$ orbits. Suppose the parameters of the system are set such that $\frac{F/m}{\sqrt{(\omega_0^2 - \omega^2)^2 + \omega^2\gamma^2}} = \sigma$. This constitutes a steady state grazing orbit. Suppose we look at stroboscopic time slices such that the grazing orbit grazes the boundary at $t = \tau$. Now we perturb the system slightly so that the system hits the boundary with some non zero velocity at $t = \tau + \delta t$

Before collision:

$$\begin{pmatrix} x(0) \\ v(0) \end{pmatrix} = \begin{pmatrix} x_p(0) \\ v_p(0) \end{pmatrix} + \begin{pmatrix} x_h(0) \\ v_h(0) \end{pmatrix}$$

$$\begin{pmatrix} x(\tau + \delta t) \\ v(\tau + \delta t) \end{pmatrix} = \begin{pmatrix} x_p(\tau + \delta t) \\ v_p(\tau + \delta t) \end{pmatrix} + \begin{pmatrix} x_h(\tau + \delta t) \\ v_h(\tau + \delta t) \end{pmatrix}$$

After collision:

$$
\begin{aligned}
\begin{pmatrix} x \\ v \end{pmatrix} &= \begin{pmatrix} x_p(\tau + \delta t) \\ -v_p(\tau + \delta t) \end{pmatrix} + \begin{pmatrix} x_h(\tau + \delta t) \\ -v_h(\tau + \delta t) \end{pmatrix} \\
&= \begin{pmatrix} x_p(\tau + \delta t) \\ v_p(\tau + \delta t) \end{pmatrix} + \begin{pmatrix} x_h(\tau + \delta t) \\ v_h(\tau + \delta t) \end{pmatrix} \\
&\quad + \begin{pmatrix} 0 \\ -2v_h(\tau + \delta t) - 2v_p(\tau + \delta t) \end{pmatrix} \begin{pmatrix} x(T) \\ v(T) \end{pmatrix} \\
&= \vec{x_p}(T) + M(T - \tau - \delta t) \left\{ \begin{pmatrix} x_h(\tau + \delta t) \\ v_h(\tau + \delta t) \end{pmatrix} \right. \\
&\quad \left. + \begin{pmatrix} 0 \\ -2v_h(\tau + \delta t) - 2v_p(\tau + \delta t) \end{pmatrix} \right\} \\
&= \vec{x_p}(T) + M(T)\vec{x_h}(0) \\
&\quad + M(T - \tau - \delta t) \begin{pmatrix} 0 \\ -2v_p(\tau + \delta t) - 2v_h(\tau + \delta t) \end{pmatrix}
\end{aligned}
$$

Where

$$
M(t) = \frac{e^{-\gamma t/2}}{\omega_g} \begin{pmatrix} \omega_g \cos \omega_g t + \frac{\gamma}{2} \sin \omega_g t & \sin \omega_g t \\ -k \sin \omega_g t & \omega_g \cos \omega_g t - \frac{\gamma}{2} \sin \omega_g t \end{pmatrix} \tag{2.7}
$$

and $(\omega_g = \frac{\sqrt{4k - \gamma^2}}{2})$

Therefore we have our Poincare map:

$$
\vec{x'}(T) = M(T)\vec{x'}(0) + M(T - \tau - \delta t) \begin{pmatrix} 0 \\ -2v_p(\tau + \delta t) - 2v_h(\tau + \delta t) \end{pmatrix} \tag{2.8}
$$

$$
\left\{ \vec{x'}(t) = \vec{x}(t) - \vec{x_p}(t) \right\}
$$

Now we draw attention to the fact that in the Poincaré map (2.8) , the second term is the actual nonlinear term.

If we can find expressions for $\delta t, v_p, v_h$ in terms of $x(0), v(0)$, the job will be done.

Let the parameters be such that the stable orbit grazes slightly: $x_m(\{parameters\}) = \sigma + \varepsilon$.

Now start from an initial condition such that $|x'(0)| = 0$. (Exactly on the stable orbit).

Then we have:

$$x_m cos\left(\omega\tau + tan^{-1}\frac{\omega\gamma}{\omega^2 - \omega_0^2}\right) = \sigma$$

$$\omega\tau + tan^{-1}\frac{\omega\gamma}{\omega^2 - \omega_0^2} = cos^{-1}\left(1 + \frac{\varepsilon}{\sigma}\right)^{-1}$$

$$\approx 2n\pi + \sqrt{\frac{2\varepsilon}{\sigma}}$$

$$\tau \approx \frac{1}{\omega}\left(2\pi + \sqrt{\frac{2\varepsilon}{\sigma}} - tan^{-1}\frac{\omega\gamma}{\omega^2 - \omega_0^2}\right)$$

Now suppose $0 < |x'(0)| << 1$. Let the time of collision $t_c = \tau + \delta t$

$$x_m cos\left(\omega(\tau + \delta t) + tan^{-1}\frac{\omega\gamma}{\omega^2 - \omega_0^2}\right) + x_h(\tau + \delta t) = \sigma$$

$$x_m cos\left(\left(\omega\tau + tan^{-1}\frac{\omega\gamma}{\omega^2 - \omega_0^2}\right) + \omega\delta t\right) + x_h(\tau + \delta t) = \sigma$$

$$\sigma - \omega x_m \delta t sin\left(\omega\tau + tan^{-1}\frac{\omega\gamma}{\omega^2 - \omega_0^2}\right) + x_h(\tau + \delta t) = \sigma$$

$$-\omega\delta t x_m\sqrt{1 - (\sigma/x_m)^2} + x_h(\tau + \delta t) = 0$$

$$\frac{x_h(\tau)}{\omega\sqrt{x_m^2 - \sigma^2} - v_h(\tau)} = \delta t$$

$$v_p(\tau + \delta t) = -\omega x_m sin\left(\omega(\tau + \delta t) + tan^{-1}\frac{\omega\gamma}{\omega^2 - \omega_0^2}\right)$$

$$= -\omega x_m sin\left(2\pi + \sqrt{\frac{2\varepsilon}{\sigma}} - tan^{-1}\frac{\omega\gamma}{\omega^2 - \omega_0^2} + \omega\delta t + tan^{-1}\frac{\omega\gamma}{\omega^2 - \omega_0^2}\right)$$

$$= -\omega x_m sin\left(\omega\delta t + \sqrt{\frac{2\varepsilon}{\sigma}}\right)$$

Using this Poincaré map, we can very easily plot the bifurcation diagrams.

Fig 2.2 and Fig 2.3 clearly demonstrates the curious effect on grazing bifurcations of making $n = \frac{2\omega_g}{\omega}$ an integer. In the non-integral case, as [?, ?] predicts, there is a chaotic region. But for $n = 2$, no such thing happens. Instead we see two fixed points immediately gaining stability.

2.3   Numerical computation of the fixed points

We see that in case of both integral n and non-integral n, a little bit after grazing periodic orbits emerged. We decided to take a look at the phase space trajectories. One such trajectory in case of $n = 2$ is plotted in Fig 2.4

Figure 2.2: Bifurcation digram for $n = 2.235$, notice the brief region of chaos after grazing
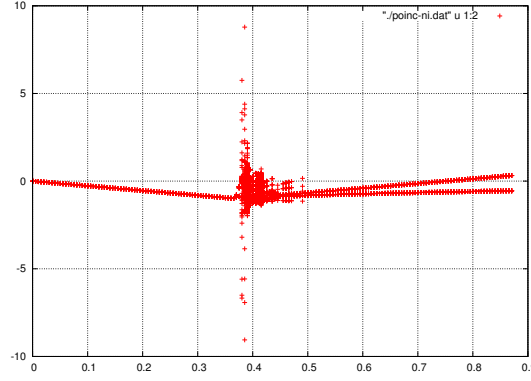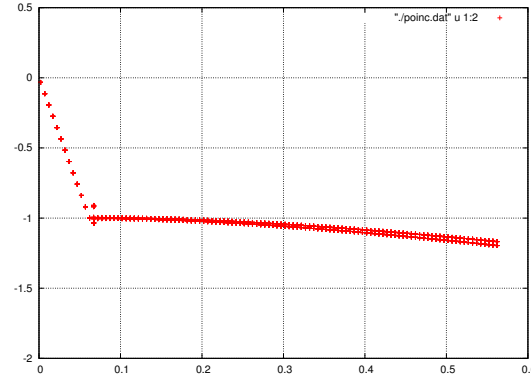

Figure 2.3: Bifurcation diagram for $n = 2$, notice the absence of chaos on grazing

As we can clearly see, this is a closed orbit involving a single collision. The time period is $2T = 2\frac{2\pi}{\omega}$. Therefore the Newton-Raphson method described in Subsection 1.4.4 would work fine for stability analysis of such orbits.

2.3.1 Numerical computation of the fixed points

We start by defining a 5-dim vector $y = (x_0, v_0, x_c, v_c, \tau)$, where τ is the time when a trajectory starting from $(x, v) = (x_0, v_0)$ collide with the hard wall and $(x, v) = (x_c, v_c)$ at that time.

Figure 2.4: $P2C1$ orbit after grazing
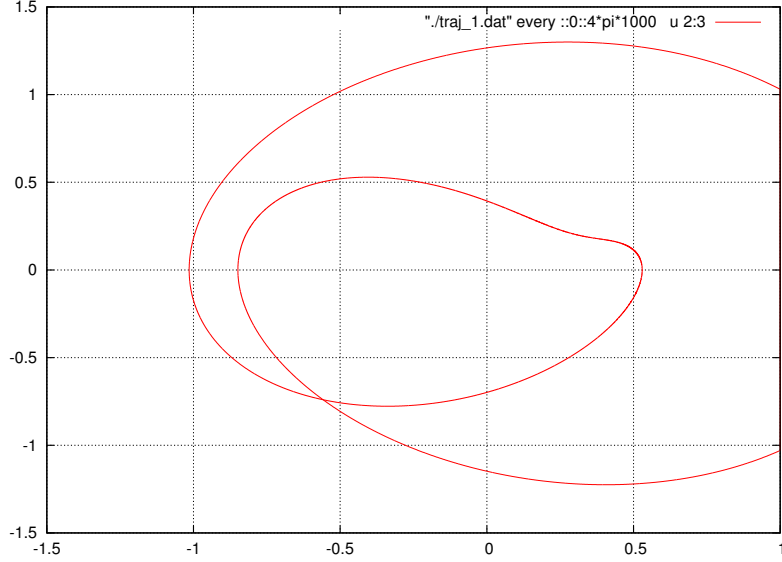
Then we get a system of equations $\mathbf{G}(y) = \mathbf{0}$ where:

$$G_{1,2}(y) = \vec{x_1} - \varphi(\tau, 0, \vec{x_0}) = 0$$
$$G_{3,4}(y) = \vec{x_0} - \varphi(2T, \tau, \vec{x_1}) = 0$$
$$G_5(y) = x_1 - \sigma = 0$$

Since this is a set of 5 equations in 5 unknowns, we can solve the equation $G(y) = 0$ using Newton-Raphson method:

$$y_{n+1} = y_n + J(y)^{-1}G(y)$$

The solution will provide us with a $P2C1$ orbit. It should be noted that this method will give *stable and unstable* orbits, unlike normal simulations which will never give us unstable orbits. However, in order to get all existing orbits, one must run the program with many initial conditions to ensure that the Newton-Raphson iteration scheme 'finds' all the solutions.

In Fig 2.5, we plot the results of such numerical calculation in the case of $n = 2.235$. We can easily see that when F is quite larger than the grazing condition (0.3903, to be exact), all the eigenvalues are < 1 in magnitude. But as the F value approaches grazing , the absolute value of one or more eigenvalues of the fixed point exceeds 1. We know from basic dynamical systems theory that this signifies the transition of the fixed point from attractor to repeller (if the magnitudes of both eigenvalues turn > 1) or saddle (if the magnitude of only one eigenvalue turn > 1).

Figure 2.5: Modulus Eigenvalues of the fixed points vs. the amplitude of the driving force for $n = 2.235$
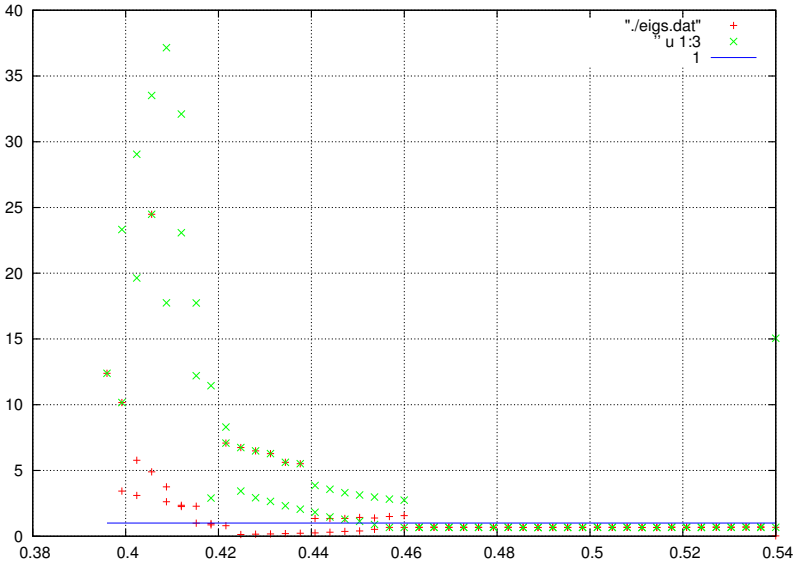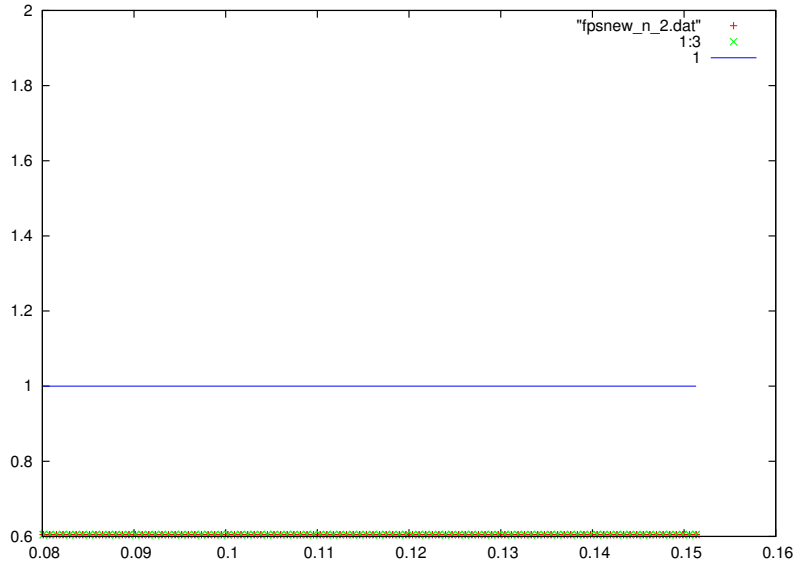

Figure 2.6: Modulus Eigenvalues of the fixed points vs. the amplitude of the driving force for $n = 2$

However, in Fig 2.6, we plot the results of such numerical calculation in the case of $n = 2$. As opposed to the previous case, no transition of the fixed point from an attractor to saddle/repeller takes place here: the eigenvalue stays put < 1 throughout the range of parameter values. This again, provides a justification for the vanishing of chaos as predicted in [?] .

However, there are a few problems in the Newton-Raphson approach of stability analysis. First of all, the numerically computed eigenvalues fluctuate a lot near grazing, possibly due to numerical errors in the Newton-Raphson iteration scheme. Secondly, it does not provide us with analytical expressions for either the fixed points or the eigenvalues, making the task of gaining physical insights into the problem much more difficult.

Therefore we decide to explore another approach for studying the same phenomena.

2.4   Impact map and its Jacobian

We had talked about the concept of impact maps in subsection subsec-impact-map. Now we will apply it in order to tackle the problem of stability analysis of single collision orbits in hard impacting oscillators.

Figure 2.7: Impact map in case of $PnC1$ orbit
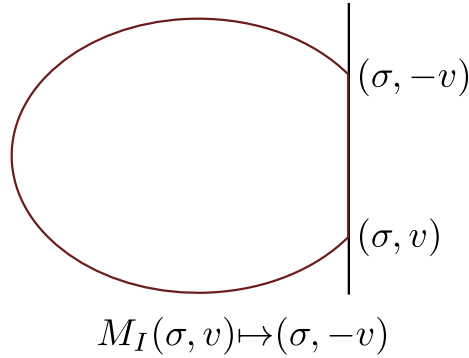
Suppose the oscillator collides against the hard wall at time τ and the state vector immediately before collision be $\begin{pmatrix} x^-(\tau) \\ v^-(\tau) \end{pmatrix}$. Just after the collision, the state vector becomes

$$\begin{pmatrix} x^+(\tau) \\ v^+(\tau) \end{pmatrix} = \begin{pmatrix} x^+(\tau) \\ -v^+(\tau) \end{pmatrix}$$

By construction, $x^-(\tau) = x^+(\tau) = \sigma$. Then we have:

$$\begin{pmatrix} x^-(\tau) \\ v^-(\tau) \end{pmatrix} = \begin{pmatrix} x_p(\tau) \\ v_p(\tau) \end{pmatrix} + \begin{pmatrix} x_h(\tau) \\ v_h(\tau) \end{pmatrix} \tag{2.9}$$

$$\begin{pmatrix} x^+(\tau) \\ v^+(\tau) \end{pmatrix} = \begin{pmatrix} x_p(\tau) \\ v_p(\tau) \end{pmatrix} + \begin{pmatrix} x_h(\tau) \\ -v_h(\tau) - 2v_p(\tau) \end{pmatrix} \tag{2.10}$$

$$\begin{pmatrix} x^-(\tau + nT) \\ v^-(\tau + nT) \end{pmatrix} = \begin{pmatrix} x_p(\tau + nT) \\ v_p(\tau + nT) \end{pmatrix} + M(nT) \begin{pmatrix} x_h(\tau) \\ -v_h(\tau) - 2v_p(\tau) \end{pmatrix} \tag{2.11}$$

$$= \begin{pmatrix} x_p(\tau) \\ v_p(\tau) \end{pmatrix} + M(nT) \begin{pmatrix} x_h(\tau) \\ -v_h(\tau) - 2v_p(\tau) \end{pmatrix} \tag{2.12}$$

Where $M(t)$ is given by (2.7).
Provided a $PmC1$ orbit exists (stable or unstable),

$$M(mT) \begin{pmatrix} x_h(\tau) \\ -v_h(\tau) - 2v_p(\tau) \end{pmatrix} = \begin{pmatrix} x_h(\tau) \\ v_h(\tau) \end{pmatrix}$$

and

$$x_p(\tau) + x_h(\tau) = \sigma$$

We recall:

$$x_p(t) = A^{[1]} cos(\omega t + tan^{-1} \frac{\omega \gamma}{\omega^2 - \omega_0^2})$$

$$v_p(t) = -A\omega sin(\omega t + tan^{-1} \frac{\omega \gamma}{\omega^2 - \omega_0^2})$$

$$= \mp A\omega \sqrt{1 - \left(\frac{x_p}{A}\right)^2}$$

$$= \mp A\omega \sqrt{1 - \left(\frac{\sigma - x_h}{A}\right)^2}$$

The condition for existence of a $PnC1$ orbit:

$$M(mT) \begin{pmatrix} x \\ -v \pm 2\omega \sqrt{A^2 - (\sigma - x_h)^2} \end{pmatrix} = \begin{pmatrix} x \\ v \end{pmatrix} \tag{2.13}$$

The uncertainty about the $\pm$ sign is a direct consequence of the fact that for the same position, the velocity of the oscillator can have two values equal in magnitude but with opposite signs.
Suppose

$$M(mT) = \begin{pmatrix} a & b \\ c & d \end{pmatrix}$$

---

[1] $A = \dfrac{F/m}{\sqrt{(\omega_0^2 - \omega^2)^2 + \omega^2 \gamma^2}}$

$$x = ax - bv \pm 2b\omega\sqrt{A^2 - (\sigma - x)^2} \qquad (2.14)$$

$$v = cx - dv \pm 2d\omega\sqrt{A^2 - (\sigma - x)^2} \qquad (2.15)$$

v can be easily eliminated:

$$\frac{x(1-a) + bv}{b} = \frac{v(1+d) - cx}{d}$$

$$bv = x(d - ad + bc)$$

Substituting in (2.14):

$$x(a - d + ad - bc - 1) \pm 2b\omega\sqrt{A^2 - (\sigma - x)^2} = x$$

$$A^2 - (\sigma - x)^2 - \left\{\frac{(a - d + ad - bc - 1)}{2b\omega}\right\}^2 x^2 = 0$$

Let

$$\alpha = \frac{(a - d + ad - bc - 1)}{2b\omega}$$

Then:

$$A^2 - (\sigma - x)^2 = \alpha^2 x^2$$

$$x^2(\alpha^2 + 1) - 2\sigma x + (\sigma^2 - A^2) = 0$$

Therefore we have the solution:

$$x^* = \frac{\sigma \pm \sqrt{\sigma^2 - (\alpha^2 + 1)(\sigma^2 - A^2)}}{\alpha^2 + 1} \qquad (2.16)$$

$$v^* = \frac{(d - ad + bc)x^*}{b} \qquad (2.17)$$

One important property of (2.16) is very evident: At grazing, $A = \sigma$. Therefore there exists a trivial solution: $(x^*, v^*) = (0, 0)$. This, of course, corresponds to a non-colliding orbit. Now, after grazing, two solutions exist simultaneously. The question is, are they attractors, repellers or saddles? This is the question we will tackle next.

In Fig 2.8, we plot the eigenvalues of the Jacobian at the fixed points obtained via Formula (2.16) against the driving force amplitude for various n values. We observe that for $n = 2.01$, all the eigenvalues at both the fixed points remain always < 1 in magnitude, even right after grazing. This means that both the fixed points are attractors.

However, for $n = 2.1$, one fixed point is an attractors throughout the whole range of parameter values. However, another one is a saddle and one of its eigenvalues shoots up as the system approaches grazing, signifying high stretching of the phase space.

In case of $n = 2.2$, both of them are repellers. Only near grazing, one of them become a saddle.

Figure 2.8: Eigenvalues of fixed points Vs. F for $n = 2.01, 2.1, 2.2$
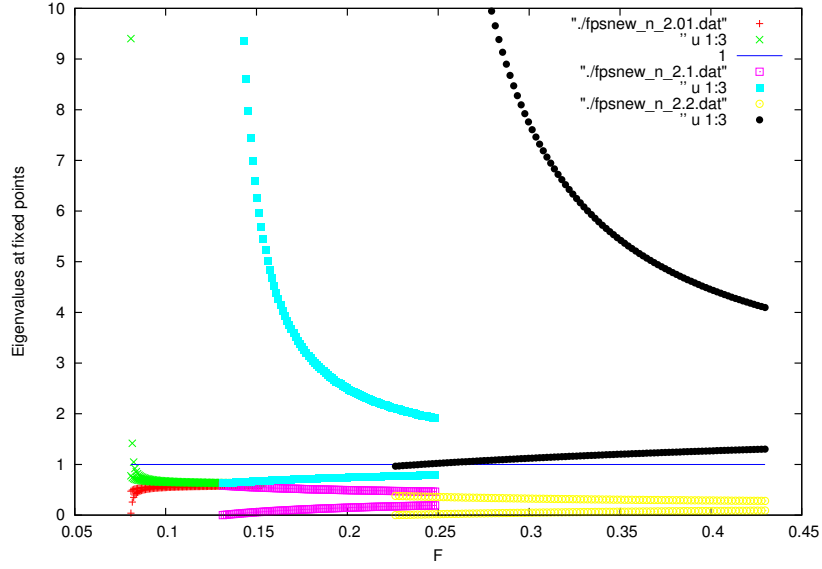
Figure 2.9: Eigenvalues of fixed points at grazing Vs. n
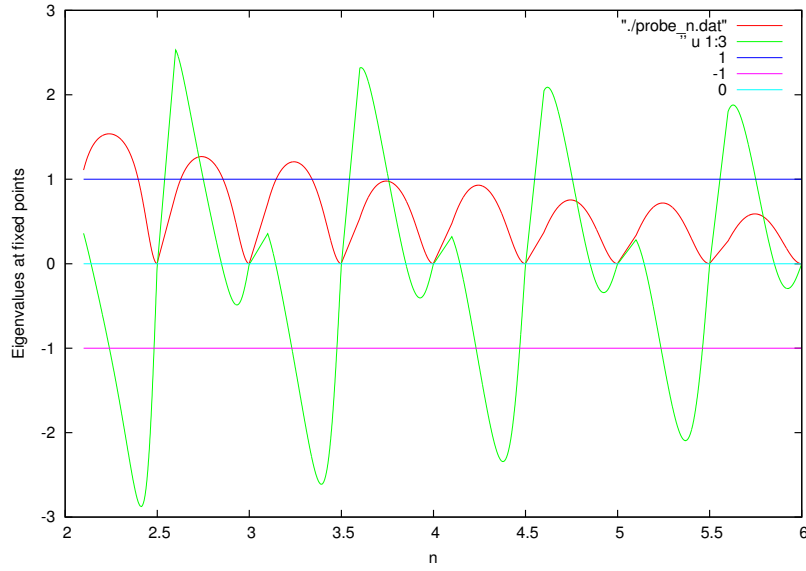
2.5   Long transients

It has previously been observed that in a system exhibiting grazing bifurcations, the time spent by it before settling down to its attractor follows a power law pattern, with a blow up at the parameter value for grazing. We have observed similar results in case of the system investigated in the last section, as depicted in Fig 2.10 and Fig 2.11.

Figure 2.10: Average transient lifetime Vs. F in the hard impacting oscillator
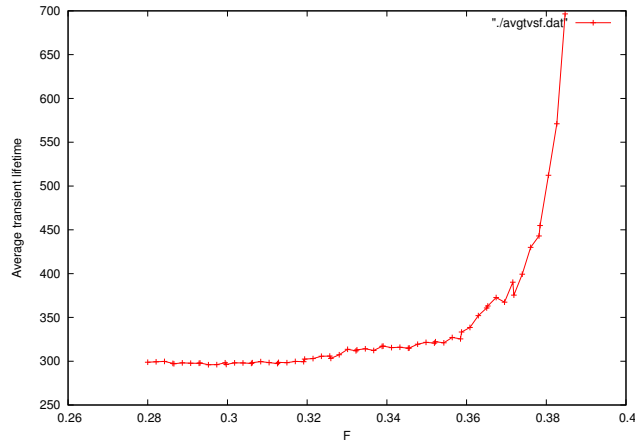
Figure 2.11: Average transient lifetime Vs. γ in the hard impacting oscillator
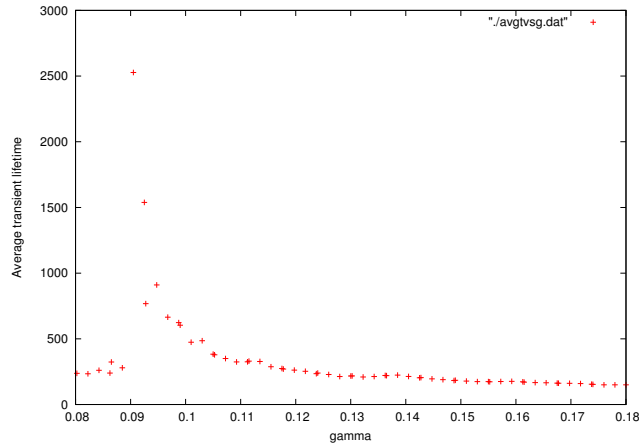
We point out here that these extra long lived transients are totally artefacts
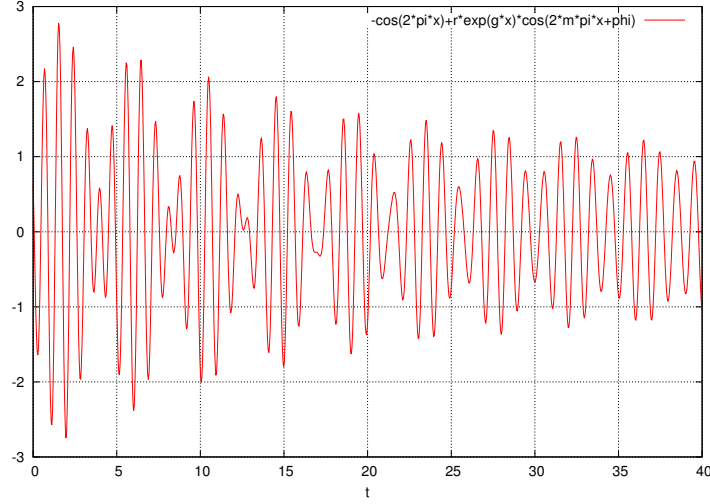
of the nonlinearity imposed by the impacts. Because without the impacts, the transient solution (which we have been calling *homogeneous solution* so far), goes as
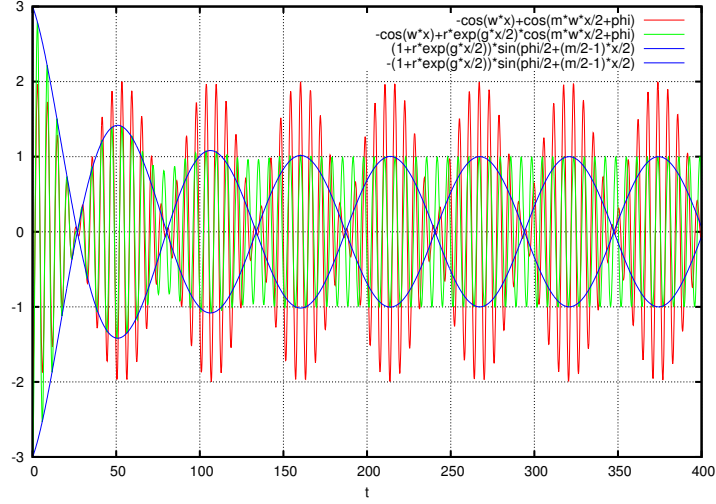
$$x_h(t) = \frac{e^{-\gamma t/2}}{\omega_g} \left\{ (\omega_g \cos \omega_g t + \frac{\gamma}{2} \sin \omega_g t)x_0 + (\sin \omega_g t)v_0 \right\} \tag{2.18}$$

Consider an initial condition:[2]

$$\vec{x_p}(0) = (-A, 0)$$
$$\vec{x_h}(0) = (x_0, v_0)$$

Where $A = \frac{F}{\sqrt{(\omega_0^2 - \omega^2)^2 + \omega^2 \gamma^2}}$

Starting from this point, the solution is, as usual:

$$x(t) = -A \cos \omega t + \frac{e^{-\gamma t/2}}{\omega_g} \left\{ (\omega_g \cos \omega_g t + \frac{\gamma}{2} \sin \omega_g t)x_0 + (\sin \omega_g t)v_0 \right\}$$

$$x(t) = -A \cos \omega t + \frac{e^{-\gamma t/2}}{\omega_g} \left\{ (\omega_g \cos \omega_g t + \frac{\gamma}{2} \sin \omega_g t)x_0 + (\sin \omega_g t)v_0 \right\}$$

$$= -A \cos \omega t + e^{-\gamma t/2} B \cos(\omega_g t + C)$$

$$C = -tan^{-1} \frac{\frac{\gamma}{2\omega_g}x_0 + \frac{v_0}{\omega_g}}{x_0}$$

$$B = \sqrt{x_0^2 + \left(\frac{\gamma}{2\omega_g}x_0 + \frac{v_0}{\omega_g} \right)^2}$$

---

[2]Taking a slice through the time dimension

In general, the sum of two different sine waves differing both in amplitude and frequency cannot be further simplified. However, an approximate envelope can be calculated.

Now the job is simple:

1. Consider the $x_0 \times v_0$ space.

2. For any point in the space, using the envelope, predict if there will be any future collision or not.

3. Points for which there is no further collision should form a closed area in the whole space.

4. The area must shrink as we approach grazing.

5. Correlate the area with transient lifetime.

The trajectory:

$$x(t) = -A \cos \omega t + e^{-\gamma t/2} B \cos\left(\omega_g t + C\right) \tag{2.19}$$

Will have an envelope:[3]

$$E(t) = \left\{ A + B e^{-\gamma t/2} \right\} \sin\left(\frac{C + (\omega_g - \omega)t}{2} \right) \tag{2.20}$$

If $\omega \approx \omega_g$

---

[3]There are some aberrations in the first bulge of the envelope

The next peak of the envelope occurs at

$$t_c = \begin{cases} \frac{\pi - C}{\omega_g - \omega} & \text{if } \omega_g > \omega \\ \frac{\pi + C}{\omega - \omega_g} & \text{if } \omega_g < \omega \end{cases} \tag{2.21}$$

And has height:

$$E_m = A + Be^{-\gamma t_c/2} \tag{2.22}$$

Definition 2.5.1. $E_m =$ *height of the next peak of the envelope.*

Definition 2.5.2. $x_m =$ *height of the next peak of the trajectory* [4]

Definition 2.5.3. $\mu_{xv} = \{(x,v) \in \mathbb{X} \times \mathbb{V} : x_m(x,v) < \sigma\}$

$$t_c \leq \frac{3\pi/2}{|\omega_g - \omega|} \tag{2.23}$$

$$x_m \geq E_m \tag{2.24}$$

$$E_m \geq A + Be^{-\gamma \frac{3\pi/4}{|\omega_g - \omega|}} \tag{2.25}$$

$$B \geq max\left\{ |x_0|, \left| \frac{\gamma}{2\omega_g} x_0 + \frac{v_0}{\omega_g} \right| \right\} \tag{2.26}$$

$$\mu_{xv} \leq \left\{ (x,v) : B \leq (\sigma - A)e^{\gamma \frac{3\pi/4}{|\omega_g - \omega|}} = \chi \right\} \tag{2.27}$$

$$\leq \left\{ (x,v) : -\chi \leq x \leq \chi, -\chi\omega_g - \frac{\gamma x}{2} \leq v \leq \chi\omega_g - \frac{\gamma x}{2} \right\} \tag{2.28}$$

2.6 No-collision area

Celso Grebogi, Edward Ott, James A. Yorke, Critical Exponent of Chaotic Transients in Nonlinear Dynamical Systems, Phys. Rev. Lett. 57, 1284–1287 (1986):

- $\tau \sim (\alpha - \alpha_*)^{-\gamma}$, γ the "critical exponent" depends on the system.

- Derives expression for γ in terms of the eigenvalues of the fixed points at collision.

Drawing parallels between the behaviour of μ_{xv} and the previous result, we can surmise:

$$\mu_{xv} \sim \frac{1}{\tau}$$

So far, we have calculated μ_{xv} by means of a Monte Carlo integration: we chose N initial points, evaluated the number n of them that does not lead to

---

[4]Except in some cases, $x_m = E_m$
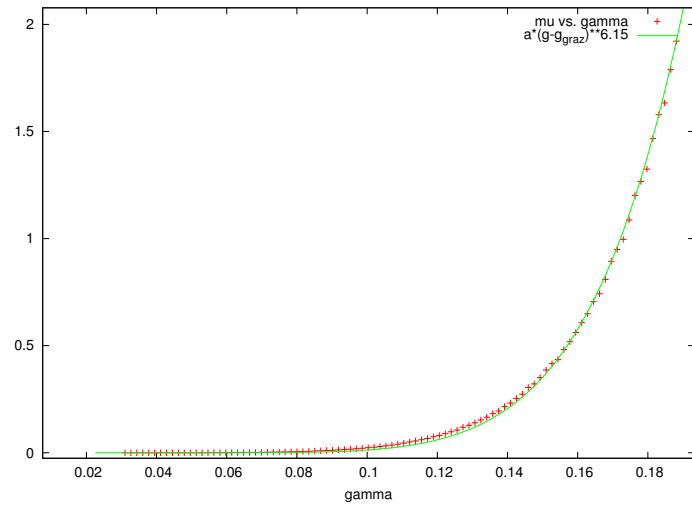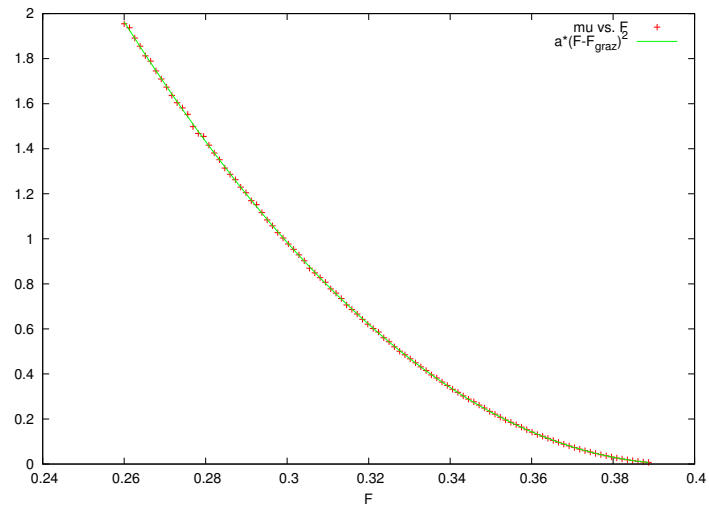
collision and equated $\frac{n}{N}$ to μ_{xv}.

Now we'll try an analytical approach.

$$\mu_{xv} = \int_{A+B(x,v)e^{-\gamma t_c(x,v)/2} < \sigma} dxdv$$

Now we recall (2.21)

$$t_c = \begin{cases} \frac{\pi - C}{\omega_g - \omega} & \text{if } \omega_g > \omega \\ \frac{\pi + C}{\omega - \omega_g} & \text{if } \omega_g < \omega \end{cases} \tag{2.29}$$

Where $C = -tan^{-1} \frac{\frac{\gamma}{2\omega_g}x_0 + \frac{v_0}{\omega_g}}{x_0}$.

Since C is a rapidly varying function of both x and v and has range $\{-\pi/2, \pi/2\}$, we can replace $C \approx 0$ without too much error.

Therefore

$$\mu_{xv} \sim \int_{A+B(x,v)e^{-\gamma \pi/(2|\omega_g - \omega|)} < \sigma} dxdv$$

$$= \int_{B(x,v) < (\sigma - A)e^{\gamma \pi/(2|\omega_g - \omega|)}} dxdv$$

Now we recall that $B = \sqrt{x_0^2 + \left(\frac{\gamma}{2\omega_g}x_0 + \frac{v_0}{\omega_g}\right)^2}$.

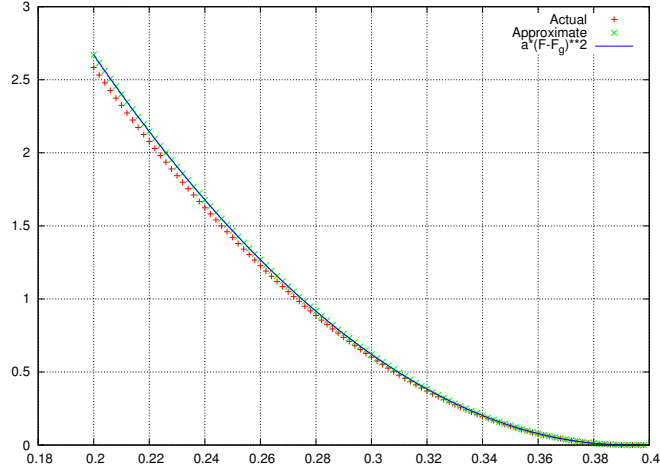So our integral is now of the form: $\int_{x^2 + (ax+by)^2 < \chi^2} dxdv$

$$\int_{x^2 + (ax+by)^2 < \chi^2} dxdy$$

$$= \int_{-\chi}^{\chi} dx \int_{x^2 + (ax+by)^2 < \chi^2} dy$$

$$= \int_{-\chi}^{\chi} \frac{\sqrt{(2abx)^2 - 4b^2(x^2(1 + a^2) - \chi^2)}}{b^2} dx$$

$$= \frac{1}{b^2} \int_{-\chi}^{\chi} 2b\sqrt{\chi^2 - x^2} dx$$

$$= \frac{2}{b} \int_{-\chi}^{\chi} \sqrt{\chi^2 - x^2} dx$$

However, we have disregarded one very important restriction: $x < \sigma$, due to the hard wall.

So, actually:

$$\mu_{xv} = 2\omega_g \int_{-\chi}^{max\{\chi,1\}} \sqrt{\chi^2 - x^2} dx$$

Figure 2.12: μ_{vx} vs. F

Recall that our calculation, both analytical and numerical, has started off with an assumption. Now we'll try to justify.

$$|f(t)cos(\omega_1 t) + g(t)cos(\omega_2 t + C)|$$
$$\leq |(f(t) + g(t))(cos(\omega_1 t) + cos(\omega_2 t + C))|$$
$$= 2\left|\{f(t) + g(t)\} \, sin\left(\frac{(\omega_1 - \omega_2)t + C}{2}\right)\right|\left|sin\left(\frac{(\omega_1 + \omega_2)t + C}{2}\right)\right|$$

Now since the last term is much more rapidly varying than the second term, we replace it with its average over a full cycle without incurring too much error:

$$= 2\left|\{f(t) + g(t)\} \, sin\left(\frac{(\omega_1 - \omega_2)t + C}{2}\right)\right| \frac{2}{\pi} \int_0^{\pi/2} cos(t)dt$$
$$= 2\left|\{f(t) + g(t)\} \, sin\left(\frac{(\omega_1 - \omega_2)t + C}{2}\right)\right| \frac{2}{\pi}$$

$\omega \gg \omega_g$

$$x(t) = -A\cos\omega t + e^{-\gamma t/2}B\cos(\omega_g t + C) \tag{2.30}$$
$$E(t) = A + e^{-\gamma t/2}B\cos(\omega_g t + C) \tag{2.31}$$

$\omega \ll \omega_g$

$$x(t) = -A\cos\omega t + e^{-\gamma t/2}B\cos(\omega_g t + C) \tag{2.32}$$
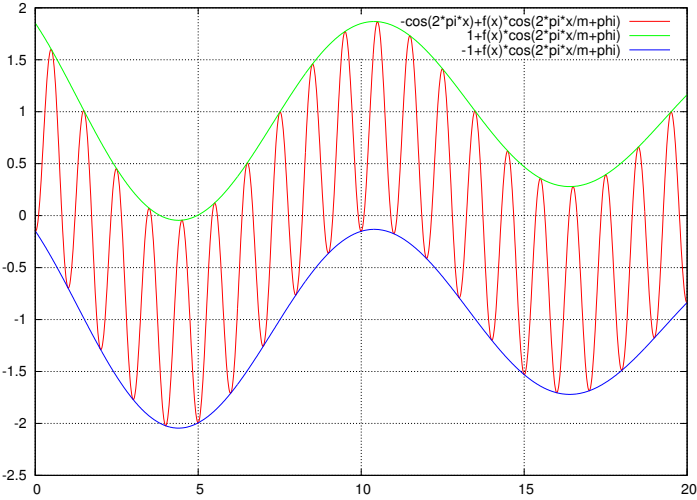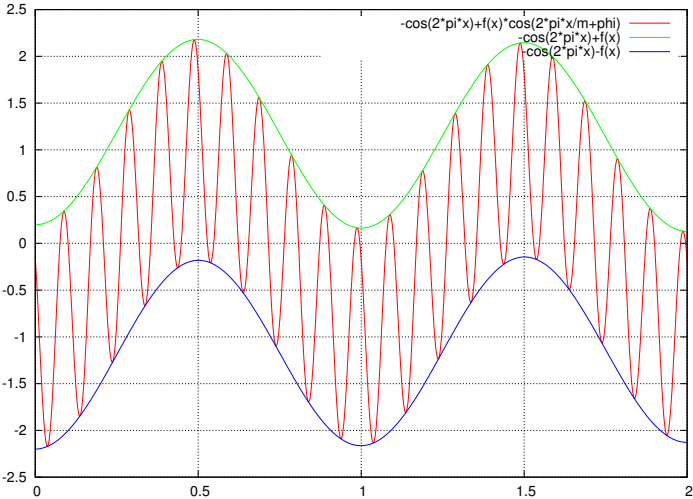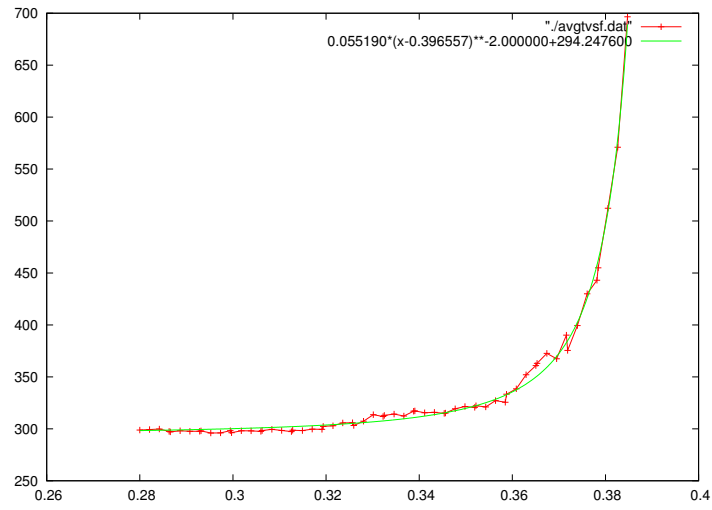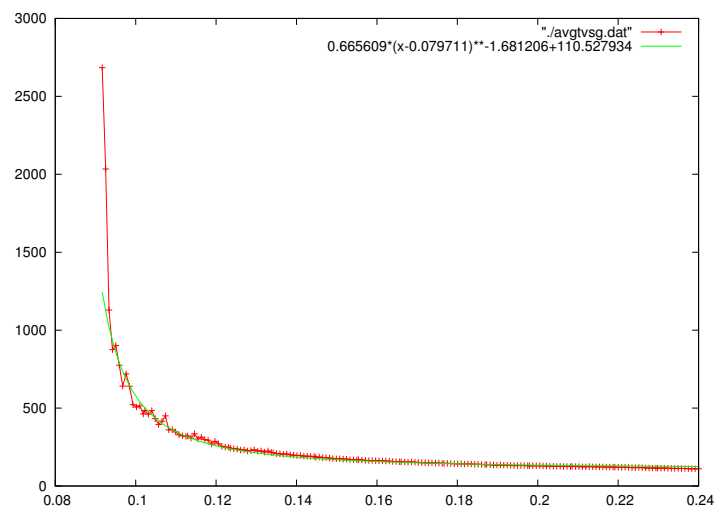$$E(t) = -A\cos\omega t + e^{-\gamma t/2}B \tag{2.33}$$

Figure 2.13: Transient lifetime vs. F

Figure 2.14: Transient lifetime vs. γ

1. Try to squeeze the parallelogram shaped bounding box of μ_{xv}.

2. Create a colourmap of $\mathbb{V} \times \mathbb{X}$ space depicting the number of cycles needed to reach stable period-1 orbit.

3. Instead of Monte Carlo integration, try a spreading-out approach.

4. As per Grebogi, Yorke et al, try to find out the "critical exponent"

5. The other extreme: $\omega_0 >> \omega$ or $\omega_0 << \omega$

6. Prove that the peak of $e^{-\gamma t/2} cos(\omega t)$ doesn't differ markedly from that of $cos(\omega t)$

Bibliography

[1] Mario Bernardo, Chris Budd, Alan Richard Champneys, and Piotr Kowalczyk. *Piecewise-smooth dynamical systems: theory and applications*, volume 163. Springer, 2007.

[2] Harry Dankowicz and Arne B Nordmark. On the origin and bifurcations of stick-slip oscillations. *Physica D: Nonlinear Phenomena*, 136(3):280–302, 2000.

[3] M Di Bernardo, CJ Budd, and AR Champneys. Grazing and border-collision in piecewise-smooth systems: A unified analytical framework. *Physical Review Letters*, 86(12):2553–2556, 2001.

[4] M Di Bernardo, M_I Feigin, SJ Hogan, and ME Homer. Local analysis of c-bifurcations in n-dimensional piecewise-smooth dynamical systems. *Chaos, Solitons and Fractals*, 10(11):1881–1908, 1999.

[5] M Di Bernardo, F Garofalo, L Iannelli, and F Vasca. Bifurcations in piecewise-smooth feedback systems. *International Journal of Control*, 75(16-17):1243–1259, 2002.

[6] M. Feigin. Doubling of the oscillation period with C-bifurcations in piecewise-continuous systems PMM vol. 34, 1970, pp. 861-869. *Journal of Applied Mathematics and Mechanics*, 34:822–830, 1970.

[7] Mats H Fredriksson and Arne B Nordmark. Bifurcations caused by grazing incidence in many degrees of freedom impact oscillators. *Proceedings of the Royal Society of London. Series A: Mathematical, Physical and Engineering Sciences*, 453(1961):1261–1276, 1997.

[8] Celso Grebogi, Edward Ott, and James A Yorke. Critical exponent of chaotic transients in nonlinear dynamical systems. *Physical review letters*, 57(11):1284–1287, 1986.

[9] R. Hilborn. *Chaos and nonlinear dynamics: an introduction for scientists and engineers*. Oxford University Press, Incorporated, 2000.

[10] Soumya Kundu, Soumitro Banerjee, and Damian Giaouris. Vanishing singularity in hard impacting systems. *Discr. Contin. Dyn. Syst., Ser. B*, 16(1):319–332, 2011.

[11] Soumya Kundu, Soumitro Banerjee, Ekaterina Pavlovskaia, Marian Wierci-
     groch, et al. Singularities in soft-impacting systems. *Physica D: Nonlinear
     Phenomena*, 241(5):553–565, 2012.

[12] Yue Ma, Soumitro Banerjee, Marian Wiercigroch, Ekaterina Pavlovskaia,
     et al. The nature of the normal form map for soft impacting systems.
     International Journal of Non-Linear Mechanics, 43(6):504–513, 2008.

[13] A. Okninski and B. Radziszewski. Chaotic dynamics in a simple bouncing
     ball model. *ArXiv e-prints*, February 2010.